Proteomics Analysis of Nucleolar SUMO-1 Target Proteins upon Proteasome Inhibition*

Vittoria Matafora‡§, Alfonsina D'Amato‡§, Silvia Mori¶‖, Francesco Blasi¶‖**, and Angela Bachi‡ ‡‡

Many cellular processes are regulated by the coordination of several post-translational modifications that allow a very fine modulation of substrates. Recently it has been reported that there is a relationship between sumoylation and ubiquitination. Here we propose that the nucleolus is the key organelle in which SUMO-1 conjugates accumulate in response to proteasome inhibition. We demonstrated that, upon proteasome inhibition, the SUMO-1 nuclear dot localization is redirected to nucleolar structures. To better understand this process we investigated, by quantitative proteomics, the effect of proteasome activity on endogenous nucleolar SUMO-1 targets. 193 potential SUMO-1 substrates were identified, and interestingly in several purified SUMO-1 conjugates ubiquitin chains were found to be present, confirming the coordination of these two modifications. 23 SUMO-1 targets were confirmed by an *in vitro* sumoylation reaction performed on nuclear substrates. They belong to protein families such as small nuclear ribonucleoproteins, heterogeneous nuclear ribonucleoproteins, ribosomal proteins, histones, RNA-binding proteins, and transcription factor regulators. Among these, histone H1, histone H3, and p160 Myb-binding protein 1A were further characterized as novel SUMO-1 substrates. The analysis of the nature of the SUMO-1 targets identified in this study strongly indicates that sumoylation, acting in coordination with the ubiquitin-proteasome system, regulates the maintenance of nucleolar integrity. ***Molecular & Cellular Proteomics 8:2243–2255, 2009.***

Targeting of proteins by conjugation of Small Ubiquitin-like MOdifier (SUMO)[1] is a key mechanism for regulating many cellular processes (1, 2), for example the activity of transcription factors (3). Other regulated processes are DNA repair, protein transport, protein-protein interaction, cell cycle progression, and RNA metabolism (4–6).

SUMO proteins are ubiquitously expressed throughout the eukaryotic kingdom. Yeast, *Caenorhabditis elegans*, and *Drosophila melanogaster* carry a single SUMO gene, whereas plants and vertebrates have several SUMO genes (5). In particular, humans express four distinct SUMO family members: SUMO-1, SUMO-2, SUMO-3, and SUMO-4 (7, 8). SUMO-1 is an 11.6 kDa protein. It shares about 47% homology with SUMO-2 and SUMO-3 that, on the contrary, differ from each other only by three amino-terminal residues and form a distinct subfamily known as SUMO-2/-3 (9). Despite the low sequence homology, SUMO-1 and SUMO-2/-3 share a similar protein size, tertiary structure, and a carboxyl-terminal diglycine motif (10, 11). At the cellular level, different amounts of free SUMO-1 and SUMO-2/-3 are present. The majority of SUMO-1 in fact is conjugated to substrates, whereas the conjugation of SUMO-2/-3 is strongly induced in response to various stresses (10). Finally SUMO-1 and SUMO-2/-3 serve distinct functions as they modify different target proteins (5). Unlike SUMO-1, SUMO-2, and SUMO-3, which are ubiquitously expressed (7), SUMO-4 isoform has yet to be characterized. It seems to be expressed mainly in the kidney, lymph nodes, and spleen, but its role still remains unclear because its mature form has never been reported *in vivo* (7, 12).

Several SUMO targets are known; they are mostly nuclear proteins presenting a consensus acceptor site: ΨK*X*E (in which Ψ is an aliphatic branched amino acid and *X* is any amino acid) (5). The mutation of this site abolishes sumoylation of substrates and is commonly used to understand the biological implication of the substrate modification. Also SUMO-2/-3 present a conserved lysine in this motif, and they form polymeric SUMO chains (13, 14). SUMO-1, however, lacks this consensus site and is not thought to form chains even if recent studies demonstrate that SUMO-1 can be linked to the end of a poly-SUMO-2/-3, terminating the chain (11).

Recently two different extensions of the simple consensus SUMO acceptor site have been identified. These motifs share a negative charge next to the basic SUMO consensus site:

From the ‡Biomolecular Mass Spectrometry Unit and ¶Molecular Genetics Unit, Division of Genomics and Cell Biology, San Raffaele Scientific Institute and ‖Università Vita Salute San Raffaele, via Olgettina 58, 20132 Milan, Italy and **FIRC Institute of Molecular Oncology (IFOM), via Adamello 16, 20139 Milan, Italy

Received, February 11, 2009, and in revised form, June 4, 2009

Published, MCP Papers in Press, July 12, 2009, DOI 10.1074/mcp.M900079-MCP200

[1] The abbreviations used are: SUMO, small ubiquitin-like modifier; Arg0, [$^{12}C_6$,$^{14}N_4$]arginine; Arg10, [$^{13}C_6$,$^{15}N_4$]arginine; Aos1/Uba2, SUMO-activating enzyme subunit 1/2 (SAE1/SAE2); E3, SUMO ligase; hnRNP, heterogeneous nuclear ribonucleoprotein; IPI, International Protein Index; Lys0, [$^{12}C_6$,$^{14}N_2$]lysine; Lys8, [$^{13}C_6$,$^{15}N_2$]lysine; p160, p160 Myb-binding protein 1A; SILAC, stable isotope labeling by amino acids in cell culture; Ubc9, ubiquitin-conjugating enzyme 9; nLC, nano-LC; LTQ, linear trap quadrupole; PANTHER, Protein Analysis through Evolutionary Relationships.

one involves a phosphorylated (p) Ser and a Pro residue (ΨK*X*E*XX*pSP), and the other contains a negatively charged amino acid close to the acceptor Lys residue (5). Although many targets contain the above mentioned motifs, there are examples of substrates that do not contain these acceptor sites. The presence of a phosphorylated residue in the motif indicates that regulatory mechanisms, which can enhance or decrease the sumoylation of specific targets, may occur at the level of the target itself (15). Indeed sumoylation often acts in coordination with other post-translational modifications like acetylation, methylation, and ubiquitination (16). As discussed above, SUMO proteins are similar in three-dimensional structures. Although they do not display high sequence homology, they share the same structure of ubiquitin and a common conjugation mechanism. In fact like ubiquitination sumoylation also requires the formation of an isopeptide bond between the carboxyl-terminal Gly residue of the modifier protein and the ε-amino group of a Lys residue in the acceptor protein (5). The enzymatic cascade that mediates SUMO conjugation is similar to that of ubiquitin. The immature precursor is first processed by a specific carboxyl-terminal hydrolase that exposes the diglycine motif, and then mature SUMO proteins are activated by an ATP-dependent heterodimer of SUMO-activating enzyme subunit 1 (SAE1) and SAE2. The above dimer transfers the activated SUMO protein to the ubiquitin-conjugating enzyme 9 (Ubc9) through a transesterification reaction. Ubc9 usually acts together with an E3 ligating enzyme that catalyzes SUMO conjugation to the substrate. In contrast to the ubiquitin pathway in which an E3 enzyme is essential for conjugation, SUMO modification just requires Ubc9, which is able to bind directly to the SUMO consensus sequence and substrates, aligning them for conjugation (5, 10, 11).

Despite the similarity between SUMO and ubiquitin, the molecular consequences of these two modifications are distinct (17, 18). In some cases, such as IκBα modification, SUMO plays an antagonistic role to ubiquitin, competing for the same lysine (19). In other cases, as for NFκB essential modulator/IκB kinase γ, SUMO and ubiquitin are conjugated in a sequential manner in response to a toxic stress; in further cases SUMO may regulate protein localization, stabilizing substrate, independently from ubiquitination as for Smad4 (20–22). Cross-regulation between SUMO and ubiquitin and the possible interchange of modifiers remain unclear (23, 24). Several recent studies indicate that there is a cross-talk between ubiquitinated and SUMO-modified proteins in coordination with proteasome activity (25–27).

To gain insights into the interconnection of the SUMO and the ubiquitin-proteasome pathway, we investigated the effect of proteasome inhibition on SUMO-conjugated proteins. We analyzed the subcellular distribution of sumoylated proteins in HeLa cells upon MG132 treatment and identified SUMO-1 targets by mass spectrometric techniques. Moreover we measured the effect of MG132 on target modification by stable isotope labeling by amino acids in cell culture (SILAC), and we demonstrated that, upon proteasome inhibition, the amount of SUMO-1 species increases and accumulates in nucleolar structures (28–30). This enrichment of SUMO-1 allowed the detection of sumoylated targets at endogenous levels, although usually the abundance of sumoylated proteins is relatively low in the cell, and they are difficult to detect. Based on these data, we focused our attention on the nucleolar compartment and identified nucleolar sumoylated proteins that accumulate after proteasome inhibition. The analysis of such proteins strongly indicates that sumoylation is involved in the regulation of nucleolar dynamics.

EXPERIMENTAL PROCEDURES

Cell Culture—HeLa cells were grown in Dulbecco's modified Eagle's medium supplemented with 10% FCS and 100 units/ml penicillin and streptomycin (Invitrogen). Stable isotope labeling was carried out essentially as described previously (28) using [$^{12}C_6$,$^{14}N_4$]arginine (referred to as Arg0), [$^{12}C_6$,$^{14}N_2$]lysine (referred to as Lys0), [$^{13}C_6$,$^{15}N_4$]arginine (referred to as Arg10), and [$^{13}C_6$,$^{15}N_2$]lysine (referred to as Lys8) (Cambridge Isotope Laboratories, Cambridge, MA). Arg0-labeled cells in experiments I and II or Arg0, Lys0-labeled cells in experiment III were treated with 10 μM MG132 in DMSO overnight; Arg10-labeled cells or Arg10, Lys8-labeled cells were treated with DMSO as control. The labeled cells, for each experiment, were mixed in a 1:1 ratio (3×10^7 cells each).

Immunofluorescence—HeLa cells were grown on sterile 13-mm coverslips and then treated with 10 μM MG132 or DMSO overnight. A time course was performed, treating HeLa cells with 10 μM MG132 for 1, 6, and 12 h using DMSO as control. Comparison of SUMO-1 staining under several stresses was carried out using 0.2 μM actinomycin D (Sigma-Aldrich) for 12 h, 10 μg/ml cycloheximide (Sigma-Aldrich) for 12 h, 1 μM Velcade (bortezomib) (Millennium Pharmaceuticals, Cambridge, MA) for 12 h, 1 mM H_2O_2 (Sigma-Aldrich) for 1 h, and 10 μM MG132 for 12 h. Cells were fixed with PBS, 3.0% paraformaldehyde for 15 min at room temperature and then permeabilized with 0.2% Triton X-100, 300 mM sucrose, 20 mM Hepes, pH 7.4, 50 mM NaCl, 3 mM $MgCl_2$ for 3 min at 4 °C. HeLa cells were incubated with the indicated antibodies in blocking buffer (0.2% bovine serum albumin in PBS) for 1 h at 37 °C, rinsed with PBS, incubated with purified Alexa Fluor 488-conjugated goat anti-mouse immunoglobulin G antibodies, rinsed, and mounted with Immuno-Fluore Mounting Medium (ICN Biomedicals, Costa Mesa, CA). The nuclei were visualized by Hoechst 33258 (Sigma-Aldrich) staining for 3 min at room temperature, and then after several washes with PBS, the nucleoli were stained with 0.66 mM pyronin Y (Sigma-Aldrich). Fluorescence was visualized with an inverted fluorescence microscope (DM IRBE; Leica, Wetzlar, Germany) and captured with a TCS-NT argon/krypton confocal laser microscope (Leica).

Plasmids, His-SUMO-1 Protein, Antibodies, Purification of Nucleoli, Immunoprecipitation, Protein Electrophoresis, and Immunoblotting—The plasmid encoding His-SUMO-1 wild type was obtained by cloning SUMO-1 cDNA, kindly donated from Ronald Hay as pGEX-SUMO-1 construct (31), into pet28a vector. The plasmid encoding Ubc9, obtained by cloning Ubc9 cDNA into pet23a vector, and the plasmids encoding His-Aos1 in pet28a and Uba2 in pet11d were kind gifts from Frauke Melchior (32).

His-SUMO-1 protein was purified by Ni^{2+} beads (Qiagen, Valencia, CA) according to the manufacturer's procedure. Aos1-Uba2 complex was purified as described previously (32). The following antibodies were used: anti-SUMO-1 monoclonal antibody (21C7 from Zymed Laboratories Inc.), anti-SUMO-1 polyclonal antibody (Santa Cruz Bio-

technology, Santa Cruz, CA), anti-nucleophosmin monoclonal antibody was kindly provided by Emanuela Colombo (33), anti-ubiquitin monoclonal antibody (Santa Cruz Biotechnology), anti-lamin A/C monoclonal antibody (Santa Cruz Biotechnology), anti-α-tubulin monoclonal antibody, anti-FLAG monoclonal antibody (both from Sigma-Aldrich), and anti-histone H3 polyclonal antibody (Abcam, Cambridge, MA).

HeLa cells were separated into cytoplasmic, nuclear, nucleoplasmic, and nucleolar fractions using a previously published protocol (34–36). Purified nucleoli were lysed in 4% SDS, 50 mM Tris, pH 8.0 and then diluted to reconstitute RIPA buffer (150 mM NaCl, 1% Nonidet P-40, 0.5% deoxycholate, 0.1% SDS, 50 mM Tris, pH 8.0) supplemented with 50 mM *N*-ethylmaleimide and protease inhibitor mixture.

Nucleolar SUMO-1 target proteins were immunoprecipitated using anti-SUMO-1 monoclonal antibody that was incubated with protein G-Sepharose 4 Fast Flow beads (GE Healthcare/Amersham Biosciences) for 1 h at 4 °C. The antibody was then linked to protein G by 3,3′-dithiobis(sulfosuccinimidylpropionate) cross-linker (Pierce) according to the manufacturer's instructions. Nucleolar lysates were incubated with the antibody bound to protein G beads at 4 °C overnight. After extensive washing with RIPA buffer, immunoprecipitates were eluted in non-reducing Laemmli buffer and then in reducing buffer. SUMO-1 proteins were separated by 10% SDS-PAGE, stained with Coomassie Brilliant Blue (Bio-Rad), and excised in 24 slices for LC-MS/MS analysis.

Concerning immunoblotting experiments, proteins separated by SDS-PAGE were subsequently transferred onto nitrocellulose membranes (GE Healthcare/Amersham Biosciences). These membranes were incubated with specific antibodies as indicated.

For p160 Myb-binding protein 1A immunoprecipitation, NIH 3T3 cells were infected using a p160-FLAG retrovirus as described before (37). Then NIH 3T3 cell nuclear extracts (38) were adjusted to IBB buffer (10 mM Tris-HCl, pH 8, 0.2% Nonidet P-40, 150 mM NaCl) and precleared with protein G-Sepharose beads for 1 h at 4 °C. The clarified supernatants were incubated with M2 anti-FLAG affinity resin (Sigma-Aldrich) overnight at 4 °C. The beads were rinsed several times with IBB buffer, resuspended in Laemmli buffer, heated at 85 °C, and centrifuged at 10,000 × *g*.

In Vitro Reaction and Purification of His-SUMO-1 Target Proteins—The *in vitro* reaction was performed on HeLa extracts (38) as follows. 1.3 mg of HeLa nuclear extract and 6 mg of HeLa cytosolic extract were incubated with 100 μg of His-SUMO-1 previously bound to Ni^{2+} beads (Qiagen), 30 μg of Ubc9, 0.5 units/ml inorganic pyrophosphatase, and 10 mM ATP in sumoylation buffer (10 mM $MgCl_2$, 0.1 mM DTT, 50 mM Tris-HCl, pH 7.5) for 1 h at room temperature (39). The reaction mixture was incubated in the absence of SUMO-1 as a control. The sumoylation reactions were stopped by adding 10 mM *N*-ethylmaleimide and 50 mM imidazole in sumoylation buffer. After exhaustive washings, the His-SUMO-1-conjugated proteins were eluted from beads with 500 mM imidazole in 50 mM Tris-HCl, 150 mM NaCl. Proteins were separated by 10% SDS-PAGE, stained by silver staining (40), and excised in 34 slices for LC-MS/MS analysis. For histones, a mixture of calf thymus total histones (1 μg) or purified histone H3 (1 μg) (Sigma-Aldrich) was incubated in the presence (or absence as control) of His-SUMO-1 (1 μg), Ubc9 (10 ng), Aos1/Uba2 (150 ng), 0.5 units/ml inorganic pyrophosphatase, and 10 mM ATP in sumoylation buffer for 1 h at room temperature.

Mass Spectrometry and Data Analysis—Mass Spectrometry analysis was performed using a hybrid quadrupole time-of-flight mass spectrometer (API QStar PULSAR, PE-Sciex, Toronto, Canada) equipped with a nanoelectrospray ion source (Proxeon Biosystems, Odense, Denmark). A total of 5 μl of trypsin-digested sample was injected in a capillary chromatographic system Agilent 1100 Series equipped with a Nano Pump, Iso Pump, and Degasser (Agilent, Santa Clara, CA). Peptide mixtures were separated on a 10-cm fused silica capillary (75-μm inner diameter and 360-μm outer diameter; Proxeon Biosystems) filled with Reprosil-Pur C_{18} 3-μm resin (Dr. Maisch GmbH, Ammerbuch-Entringen, Germany) using a pressurized "packing bomb." Peptides were eluted with a 60-min gradient from 92% buffer A (2% acetonitrile, 0.2% formic acid in water) to 80% buffer B (2% water, 0.2% formic acid in acetonitrile) at a constant flow rate of 200 nl/min. Analyses were performed in positive ion mode; the high voltage potential was set at around 1.6–1.8 kV. Full-scan mass spectra ranging from *m/z* 350 to 1350 Da were collected, and for each MS spectrum, the two most intense doubly and triply charged ions peaks in the mass range were selected for fragmentation. Tandem mass spectra were extracted by Mascot.dll (version 1.6.0.21) through Analyst QS 1.1 (Applied Biosystems, Foster city, CA).

Mass spectrometry analysis was also performed by LC-MS/MS using an LTQ-Orbitrap mass spectrometer (ThermoScientific, Bremen, Germany). 5 μl of tryptic digest for each band were injected in a capillary chromatographic system (EasyLC, Proxeon Biosystems). Peptide separations occurred on a homemade column as described above. A gradient of eluents A (distilled water with 2% (v/v) acetonitrile, 0.1% (v/v) formic acid) and B (acetonitrile, 2% (v/v) distilled water with 0.1% (v/v) formic acid) was used to achieve separation from 8% B (at 0 min, 0.2 ml/min flow rate) to 50% B (at 80 min, 0.2 ml/min flow rate).The LC system was connected to the orbitrap equipped with a nanoelectrospray ion source (Proxeon Biosystems). Full-scan mass spectra were acquired in the LTQ-Orbitrap mass spectrometer in the mass range *m/z* 350 to 1500 Da and with the resolution set to 60,000. The "lock-mass" option was used for accurate mass measurements. The four most intense doubly and triply charged ions were automatically selected and fragmented in the ion trap. Target ions already selected for the MS/MS were dynamically excluded for 60 s. All MS/MS samples were analyzed using the Mascot search engine (version 2.1.04; Matrix Science, London, UK) and X! Tandem (version 2007.01.01.1; The Global Proteome Machine Organization). X! Tandem and Mascot were set up to search the IPI_human_20081019 database (total, 73,994 sequences). QStar data were searched with a peptide mass tolerance of 100 ppm and 0.4 Da for precursor and fragment ions, respectively. Searches were performed with trypsin specificity, alkylation of cysteine by carbamidomethylation as a fixed modification, and oxidation of methionine as a variable modification. For LTQ-Orbitrap data mass tolerance was set to 5 ppm and 0.4 Da for precursor and fragment ions, respectively. Scaffold (version Scaffold_2_01_02, Proteome Software Inc., Portland, OR) was used to validate MS/MS-based peptide and protein identifications. Protein probabilities were assigned by the Protein Prophet algorithm (41). Protein thresholds were set to 99.0% minimum and a two-peptide minimum, whereas peptide thresholds were set to 95% minimum. The false positive rate was estimated consulting the IPI_human/decoy database (42). The estimated false positive rate was less then 4% in accordance with the Scaffold criteria selected in this work.[2] MSQuant, an open source program (SourceForge, Inc.), was used to extract quantitative information from the Mascot HTML database search files and to manually validate the certainty in peptide identification and peptide abundance ratio. Data analysis was also performed with the MaxQuant software (44). Mass spectra were analyzed by Mascot (version 2.2.2) against a concatenated forward and reversed version of the IPI human database (IPI.HUMAN.v3.52.decoy). The initial mass tolerance in MS mode was set to 7 ppm, and MS/MS mass tolerance was 0.5 Da. Cysteine carbamidomethylation was

[2] Wilmarth, P. A., and Searle, B. C. (2006) Poster presented at the Human Proteome Organisation (HUPO) 5th Annual World Congress, Long Beach, CA (October 28–November 1, 2006).

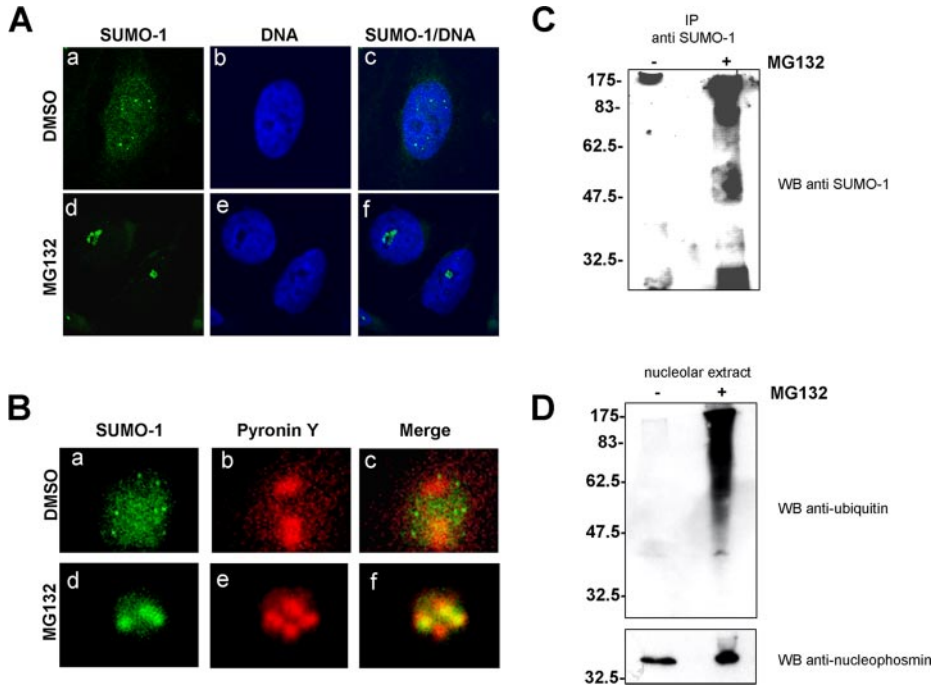

FIG. 1. **Subcellular distribution of SUMO-1 after DMSO or MG132 treatment and immunoprecipitation of nucleolar extract using anti-SUMO-1.** *A*, immunofluorescence analysis of HeLa cells cultured in the presence of DMSO as control (*a–c*) and with 10 μM MG132 overnight (*d–f*). Double staining of DNA (*blue*; Hoechst staining) and SUMO-1 (*green*) is shown in the *right panels* (*c* and *f*), the *middle panels* show DNA (*b* and *e*), and the *left panels* show SUMO-1 (*a* and *d*). In the control cells, SUMO-1 proteins are distributed throughout the nucleoplasm (*a*) excluding the nucleoli (*c*). In the treated cells, SUMO-1 proteins localize inside the nucleoli (*f*). *B*, nucleolar localization of SUMO-1 in HeLa cells treated with DMSO (*a–c*) and with MG132 overnight (*d–f*). Shown are high magnification images of SUMO-1 staining (*green*) (*a* and *d*) and pyronin Y staining (*red*) (*b* and *e*) and the merged images of pyronin Y and SUMO-1 staining (*c* and *f*). Only in HeLa cells treated with MG132 staining of SUMO-1 and pyronin Y overlaps, confirming that SUMO-1 species translocated into nucleolar structures after proteasome inhibition. *C*, immunoprecipitation (*IP*), with anti-SUMO-1 antibody, of HeLa cells nucleolar extract treated with MG132 overnight (*right*) and with DMSO (*left*). As expected SUMO-1 proteins are enriched only after proteasome inhibition. *D*, anti-ubiquitin Western blot (*WB*) of nucleolar extracts before and after MG132 treatment. The extracts were normalized with anti-nucleophosmin.

searched as a fixed modification, whereas *N*-acetyl protein and oxidized methionine were searched as variable modifications. Labeled arginine and lysine were also specified as variable modifications. The resulting Mascot ".dat" files were loaded into the MaxQuant software together with the raw data for further analysis. SILAC peptide and protein quantification was performed automatically with MaxQuant using default settings as parameters. Protein quantification was based on extracted ion chromatograms of contained peptides. Peptide assignments were statistically evaluated using a Bayesian model on the basis of sequence length and Mascot score. Peptides and proteins were accepted with a false discovery rate of less than 1%, estimated on the basis of the number of accepted reverse hits. The experiments were performed in biological triplicate (experiments I, II, and III).

RESULTS

Endogenous SUMO-1 Conjugates Accumulate in Nucleolar Structures upon Proteasome Inhibition—To examine the link between SUMO-1 and the proteasome pathway, the effect of the proteasome inhibitor MG132 on the subcellular localization of SUMO-1 was analyzed. Immunofluorescence was performed on HeLa cells treated with 10 μM MG132 overnight or DMSO as control. In the control cells, SUMO-1-positive staining was seen as dots dispersed throughout the nucleus; whereas after MG132 treatment, the staining accumulated in well defined structures (Fig. 1*A*) in agreement with previous studies (25, 26). To verify the nature of such structures, a double staining of SUMO-1 and pyronin Y, a nucleolus-specific marker, was performed. As evident from Fig. 1*B*, in treated cells SUMO-1 appears to accumulate into nucleoli. The dynamic behavior of SUMO-1 structures during proteasome inhibition was followed in HeLa cells at different times. As shown in Fig. 2, during the treatment with MG132, SUMO-1 structures increased in size and number. These new structures appear to be highly dynamic: as the treatment progressed, larger portions of SUMO-1 structures had the propensity to fuse with each other moving into the nucleolar compartment. These events resemble the fission and fusion processes of the promyelocytic leukemia bodies during chromatin organization (45). The changes of SUMO-1 structures in HeLa cells were also observed upon several stress conditions. The immunofluorescence analysis in supplemental Fig. 1 reveals that cycloheximide (26), actinomycin D (45), and oxidative stress (46) had no effect on the nucleolar accumulation of SUMO-1 particles. Conversely the behavior of

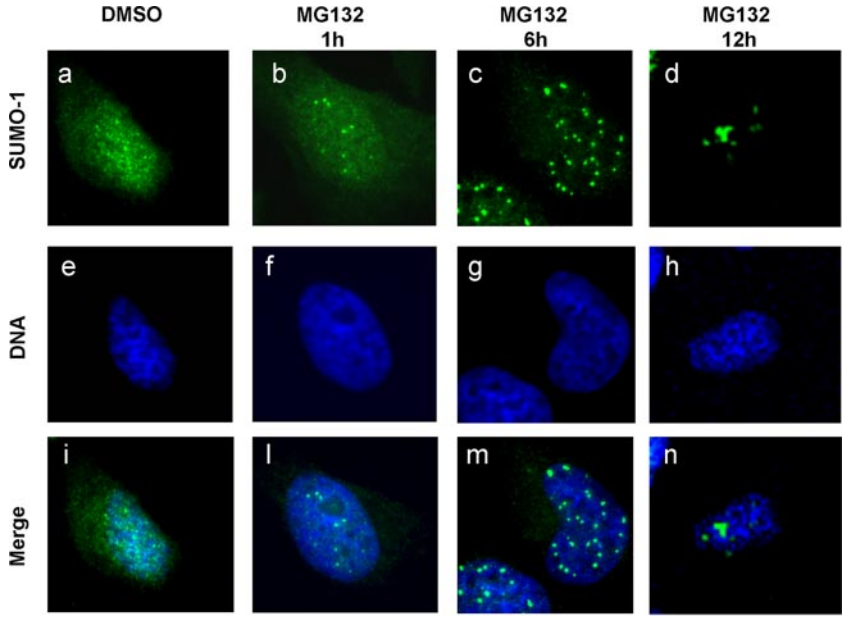

FIG. 2. **Subcellular distribution of SUMO-1 after DMSO and MG132 treatment at different time points.** Shown is immunofluorescence analysis of HeLa cells cultured in the presence of DMSO as control (*a*, *e*, and *i*) and with 10 μM MG132 for 1 h (*b*, *f*, and *l*), 6 h (*c*, *g*, and *m*), and 12 h (*d*, *h*, and *n*). Double staining of DNA (*blue*; Hoechst staining) and SUMO-1 (*green*) is shown in the *lower panels* (*i–n*), the *middle panels* show DNA (*e–h*), and the *upper panels* show SUMO-1 (*a* and *d*). As expected, in the control cells, SUMO-1 proteins are distributed throughout the nucleoplasm (*a*) excluding the nucleoli (*i*). In treated cells, SUMO-1 proteins localize first in more defined dots (*b* and *l*); after 6 h, more and bigger dots localized around the nucleoli are detected (*c* and *m*) and are finally found inside nucleolar structures (12 h) (*d* and *n*).

SUMO-1 structures after Velcade treatment, a potent and selective proteasome inhibitor (47), was the same as that observed upon MG132 treatment, confirming the specificity of the stimulus.

This observation was confirmed by biochemical analysis of purified nucleoli. Immunoprecipitation with anti-SUMO-1 antibody was used to enrich the sumoylated proteins. The Western blot analysis of treated and untreated samples shows that SUMO-1 conjugated proteins accumulated in nucleolar extract in treated cells (Fig. 1*C*). A Western blot with anti-ubiquitin was performed on the same nucleolar extracts (Fig. 1*D*) to show that, after treatment with MG132, the level of ubiquitinated protein increased, confirming the effectiveness of the inhibition.

Proteomics Analysis of Nucleolar Sumoylated Proteins—To study the effect of proteasome inhibition on endogenous SUMO-1 targets, a quantitative proteomics analysis (SILAC) on HeLa nucleolar sumoylated proteins was performed. Two different SILAC experiments were performed: one using the isotopes Arg0 and Arg10 (the two biological replicates are named SILAC I and SILAC II) and the other using Arg0, Lys0 and Arg10, Lys8 (SILAC III). In all experiments, cells grown with the light isotopes were treated with MG132, whereas the other cell population, grown with the heavy isotopes, was treated with DMSO (Fig. 3). The two HeLa populations from each SILAC experiment were mixed in a 1:1 ratio, and nucleoli were isolated. To verify the purity of the nucleolar fraction, equal amounts of proteins from cytoplasmic, nuclear, nucleoplasmic, and nucleolar fractions were immunolabeled with specific antibodies against α-tubulin, lamin A/C, and nucleophosmin. The presence of the signal of nucleophosmin and the absence of lamin A/C and α-tubulin signals in the nucleolar fraction attest the quality of the purification (supplemental Fig. S2). To purify SUMO-1-specific targets, nucleoli were

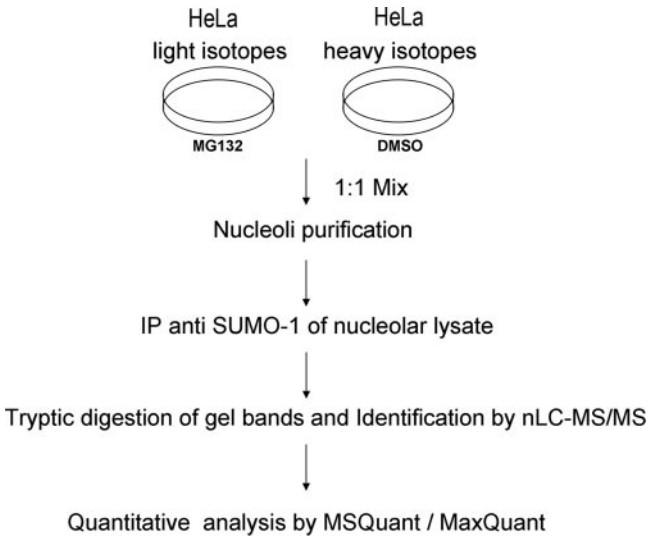

FIG. 3. **Quantitative proteomics strategy to identify nucleolar SUMO-1 targets.** Arg0- or Arg0 and Lys0-labeled HeLa cells were treated with MG132 overnight, and Arg10- or Arg10 and Lys8-labeled HeLa cells were treated with DMSO as control. Labeled cells were mixed in a 1:1 ratio, and the nucleoli were purified. SUMO-1 target proteins were immunoprecipitated (*IP*) and separated by SDS-PAGE, and the gel lane was cut into slices. Proteins were in-gel digested with trypsin, identified by mass spectrometry, and quantified by MSQuant and Max Quant.

lysed and immunoprecipitated with anti-SUMO-1 antibody (Fig. 4). 10 mM *N*-ethylmaleimide was added in the lysis buffer to inhibit SUMO proteases that remove SUMO from target proteins, and 0.5% SDS, a strong ionic detergent, was used for the immunoprecipitation to break up protein complexes and enhance the specificity of the purification. Moreover a cross-linker carrying a disulfide bridge, 3,3′-dithiobis(sulfosuccinimidylpropionate), was used to link SUMO-1 antibody to

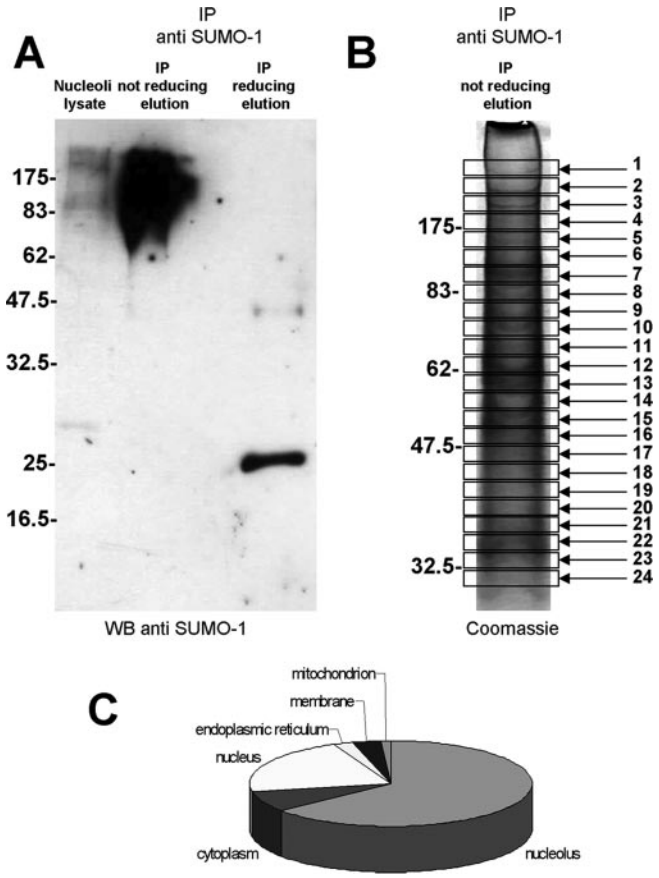

FIG. 4. **Purification of nucleolar SUMO-1 proteins.** Arg0-labeled HeLa cells were treated with MG132, and Arg10-labeled HeLa cells were treated with DMSO as control. Equal amounts of HeLa cells were mixed. SUMO-1 target proteins were immunoprecipitated (*IP*) from nucleolar lysate using anti-SUMO-1 antibody cross-linked to protein G-Sepharose beads. Immunoprecipitated proteins were eluted in non-reducing Laemmli buffer and then in reducing buffer. *A*, Western blot (*WB*) analysis shows that most of the SUMO-1 targets are eluted in non-reducing conditions. *B*, SDS-PAGE of purified SUMO-1 proteins. The gel lane was excised in 24 slices, and proteins were in-gel digested with trypsin. *C*, subcellular localization of the identified proteins.

protein G. The advantage of this step is the possibility to elute specific proteins and immunoglobulins in differential ways using non-reducing and reducing denaturing conditions (Fig. 3*A*). As expected, SUMO-1 targets were enriched after immunoprecipitation only in non-reducing conditions, indicating the validity of the purification strategy.

Eluted proteins were then separated by SDS-PAGE (Fig. 4*B*), and the top part of the Coomassie gel lane, which contains the majority of the SUMO conjugates, was cut in several slices. Proteins were in-gel digested by trypsin. The resulting peptide mixtures were analyzed by nLC-MS/MS, and only the proteins identified in at least in two of three biological replicates (193 proteins) were selected. A complete list of all identified proteins is available in supplemental Table S1. Because the SILAC technique can quantify changes as small as 10%, we chose 0.8 as a conservative cutoff ratio of heavy and light peptides, obtained by using MSQuant and MaxQuant softwares. The presence of structural proteins, potential contaminants of the mixture, such as Plectin 1, with an Arg10/Arg0 or Lys8/Lys0 ratio equal to 1 attested the validity of the quantitative analysis and excluded the implication of these proteins in the SUMO-ubiquitin pathway. In Table I are listed the proteins identified by at least two arginine- or lysine-containing peptides and enriched at least 0.8-fold in the heavy arginine or lysine form. An average of the three independently measured ratios is shown with S.D. For most potential sumoylated proteins the heavy and light peptide ratio is 0.6–0.7 with an average S.D. of 0.06 indicating that two-peptide pairs lead to reasonably accurate quantification and attesting the good reproducibility of the experiment. Moreover the potential SUMO-1 targets are listed with their subcellular localization obtained consulting the ExPASy Proteomics Server and nucleolar database (NOPdb; Ref. 36). Several potential SUMO-1 targets are nucleolar proteins, whereas the others are enriched in nucleoli after proteasome inhibition (Fig. 4*C*). Interestingly we found the ubiquitin peptide containing Lys-48 modified by the Gly-Gly moiety characteristic of polyubiquitin chain formation (supplemental Fig. S3). Ubiquitin peptides of these chains notably increase (heavy/light ratio of 0.2) in high molecular weight bands, demonstrating the accumulation of polyubiquitinated proteins after proteasome inhibition (Table I). Gene Ontology analysis of biological process was performed with the on-line software PANTHER using the data reported in Table I. As shown in Fig. 5, sumoylated targets were significantly enriched in proteins involved in ribosome biogenesis, RNA splicing and metabolism, and chromatin remodeling.

Confirming SUMO-1 Target Proteins—To validate the *in vivo* identified SUMO-1 targets, we performed an *in vitro* sumoylation reaction. In particular, we used HeLa nuclear extract as the source of SUMO-1 targets, HeLa cytosolic extract as the source of sumoylation enzymes, and an excess of His-SUMO-1, Ubc9, inorganic pyrophosphatase, and ATP as the components of the sumoylation buffer. As a control, the reaction mixture was incubated in the absence of SUMO-1. His-SUMO-1-tagged proteins were affinity purified on Ni^{2+} beads. 10% of the eluted sumoylated targets were separated by SDS-PAGE and immunoblotted using anti-SUMO-1 antibody. As shown in Fig. 6*A*, the *in vitro* reaction sharply increased the level of sumoylated proteins. The remaining part of the purified His-SUMO-1 targets was separated by SDS-PAGE. Comparing the elution with the control, the recovery of SUMO target proteins was highly specific (Fig. 6*B*). The top part of the silver-stained gel lane, which contains the majority of the SUMO-1 conjugates, was cut in several slices, and proteins were in-gel digested with trypsin. The peptide mixtures were analyzed by nLC-MS/MS, identified by database search with the Mascot search engine, and validated by Scaffold software. In Table I, *in vitro* identified SUMO-1 targets are labeled by Footnote a. A complete list of

TABLE I

Quantitative proteomics analysis of nucleolar sumoylated proteins upon proteasome inhibition

Proteins identified by at least two arginine- or lysine- containing peptides and enriched at least 0.8-fold in the heavy arginine or lysine form are shown. H/L, heavy/light ratio; FACT, facilitates chromatin transcription; TPR, translocated promoter region.

IPI accession number	Swiss-Prot accession number	Protein name	Protein score	Protein mass	Matched peptides	Protein coverage	H/L ratio			Average	S.D.	SUMO prediction sites	Subcellular localization
							Experiment I	Experiment II	Experiment III				
				Da		%							
IPI00296337	P78527	Isoform 1 of DNA-dependent protein kinase catalytic subunit[a]	2,499	473,749	79	16.1	0.79	0.63	0.5	0.64	0.15	IKSE 0.94, LKEE 0.91	Nucleoli
IPI00004970	O75691	Small subunit processome component 20 homolog	169	320,846	7	2.2	0.68	0.3		0.49	0.27	IKED 0.94, VKDE 0.93	Nucleoli
IPI00019502	P35579	Myosin-9[a,b]	1,801	227,646	42	21.8	0.82	0.65	0.66	0.71	0.10	VKND 0.93, LKTD 0.91	Nucleoli
IPI00783060	P62988	Ubiquitin	195	8,560	5	60.5	0.2	0.09	0.03	0.11	0.09	None	
IPI00007928	Q6P2Q9	Pre-mRNA-processing-splicing factor 8[a]	117	274,738	5	1.6	0.76	0.49	0.56	0.60	0.14	IKVE 0.94, IKTE 0.94	Nucleoli
IPI00009342	P46940	Ras GTPase-activating-like protein IQGAP1[a]	377	189,761	14	7.8	0.79	0.66		0.73	0.09	IKTD 0.94, VKED 0.93	Cell membrane
IPI00420014	O75643	U5 small nuclear ribonucleoprotein 200-kDa helicase[a,b]	336	246,006	11	5	0.75	0.58	0.62	0.65	0.09	VKLD 0.93, VKYD 0.93	Nucleoli
IPI00218753	P11388	Isoform 3 of DNA topoisomerase 2-α[a,b]	234	179,398	13	7.5	0.78	0.52		0.65	0.18	IKNE 0.94	Nucleus
IPI00024067	Q00610	Isoform 1 of clathrin heavy chain 1	1,032	193,260	29	15.2	0.76	0.59	0.71	0.69	0.09	IKAD 0.94, IKAD 0.94	Cytosol
IPI00005024	Q9BQG0	Isoform 1 of Myb-binding protein 1A[a]	1,012	149,731	26	16.8	0.74	0.37	0.64	0.58	0.19	VKKD 0.93, LKAD 0.91	Nucleoli
IPI00006702	Q81ZL8	Isoform 1 of proline-, glutamic acid-, and leucine-rich protein 1	160	120,879	4	3.9	0.69	0.35		0.52	0.24	IKEE 0.94, LKLD 0.91	Nucleoli
IPI00449049	P09874	Poly(ADP-ribose) polymerase 1[a]	393	113,811	8	8.6	0.87	0.47	0.8	0.71	0.21	IKDE 0.94, VKAE 0.93	Nucleus
IPI00100160	Q86VP6	Isoform 1 of Cullin-associated NEDD8-dissociated protein 1	323	137,999	10	7.2	0.81	0.7		0.76	0.08	IKLD 0.94, VKAD 0.93	Nucleus
IPI00479217	Q00839	Isoform short of heterogeneous nuclear ribonucleoprotein U[a,b]	286	89,665	7	8.8	0.77	0.69	0.72	0.73	0.04	LKEE 0.91, LKAE 0.91	Nucleus
IPI00152890	Q9H6R4	Isoform 1 of nucleolar protein 6[a]	221	128,368	7	5.4	0.74	0.35		0.55	0.28	LKDG 0.73	Nucleoli
IPI00300127	Q9H0A0	*N*-acetyltransferase 10[a]	187	116,543	7	7.5	0.74	0.67		0.71	0.05	IKQD 0.94, LKSD 0.91	Nucleoli
IPI00297211	O60264	SWI/SNF-related matrix-associated actin-dependent regulator of chromatin subfamily A	178	122,513	6	4.8	0.79	0.68		0.74	0.08	IKAD 0.94, IKNE 0.94	Nucleus
IPI00654555	Q3KQS4	NOL1 protein[a]	154	93,202	4	5.6	0.75	0.59		0.67	0.11	LKKD 0.91	Nucleoli
IPI00017297	P43243	Matrin-3[a]	152	95,078	6	8.4	0.81	0.64		0.73	0.12	IKNE 0.94, VKVD 0.93	Nucleus
IPI00140420	Q7KZF4	Staphylococcal nuclease domain-containing protein 1[a]	141	102,618	4	4.1	0.83	0.5	0.58	0.64	0.17	IKCP 0.84	Nucleus
IPI00444262	P19338	CDNA FLJ45706 fi, highly similar to nucleolin	733	65,979	13	16.7	0.62	0.56	0.71	0.63	0.08	IKLE 0.94	Nucleoli
IPI00015953	Q9NR30	Isoform 1 of nucleolar RNA helicase 2[a,b]	413	87,804	11	13.9	0.62	0.52	0.48	0.54	0.07	IKQD 0.94	Nucleoli
IPI00010740	P23246	Isoform long of splicing factor, proline- and glutamine-rich[a]	235	76,216	5	7.1	0.79	0.48	0.72	0.66	0.16	IKLE 0.94	Nucleoli
IPI00013214	P25205	DNA replication licensing factor MCM3	143	91,551	4	4.8	0.7	0.34		0.52	0.25	AKAG 0.62	Nucleoli
IPI00414676	P08238	Heat shock protein HSP 90-β[b]	825	85,104	17	19.7	0.53	0.37	0.48	0.46	0.08	LKID 0.91, LKED 0.91	Nucleoli
IPI00784295	Q2VPJ6	Heat shock protein HSP 90-α[b]	658	98,670	13	14.5	0.4	0.32	0.21	0.31	0.10	LKED 0.91, IKLG 0.77	Nucleoli
IPI00022774	P55072	Transitional endoplasmic reticulum ATPase	387	89,950	8	10.9	0.55	0.89	0.42	0.62	0.24	IKRE 0.94, VKRE 0.93	Nucleus
IPI00396435	O43143	DEAH (Asp-Glu-Ala-His) box polypeptide 15[b]	278	93,568	10	11.7	0.74	0.62	0.8	0.72	0.09	IKPE 0.94, IKRE 0.94	Nucleus
IPI00001639	Q14974	Importin β-1 subunit	208	98,420	7	9.5	0.71	0.49	0.88	0.69	0.20	LKGD 0.91	Nucleus
IPI00005154	Q08945	FACT complex subunit SSRP1[b]	200	81,367	5	6.1	0.76	0.57	0.84	0.72	0.14	IKSD 0.94, VKME 0.93	Nucleoli
IPI00306369	Q08J23	NOL1/NOP2/Sun domain family 2 protein	169	87,214	7	9.1	0.76		0.66	0.71	0.07	LKYE 0.91	Nucleoli
IPI00304925	P08107	Heat shock 70-kDa protein 1[b]	535	70,294	10	16.2	0.14	0.06	0.03	0.08	0.06	AKLD 0.79	Nucleus

TABLE I—*continued*

IPI accession number	Swiss-Prot accession number	Protein name	Protein score	Protein mass	Matched peptides	Protein coverage	H/L ratio			Average	S.D.	SUMO prediction sites	Subcellular localization
							Experiment I	Experiment II	Experiment III				
				Da		%							
IPI00003362	P11021	Isoform 1 of heat shock 70-kDa protein 5	407	71,082	11	13.5	0.62	0.52	0.67	0.60	0.08	AKFE 0.79	Nucleoli
IPI00171903	P52272	Isoform 1 of heterogeneous nuclear ribonucleoprotein M[a,b]	277	77,749	6	12.1	0.73	0.68	0.77	0.73	0.05	IKME 0.94, IKME 0.94	Nucleoli
IPI00299904	P33993	Isoform 1 of DNA replication licensing factor MCM7	225	81,884	6	8.5	0.71	0.69	0.54	0.65	0.09	FKYG 0.68	Nucleoli
IPI00013174	Q96PK6	Isoform 1 of RNA-binding protein 14[a]	109	69,620	4	4.9	0.67	0.52		0.60	0.11	None	Nucleus
IPI00021405	P02545	Isoform A of lamin A/C[a,b]	906	74,380	30	26.4	0.78	0.73	0.71	0.74	0.04	MKEE 0.80	Nucleoli
IPI00003865	P11142	Isoform 1 of heat shock cognate 71-kDa protein	459	71,082	10	12.1	0.49	0.53	0.31	0.44	0.12	AKLD 0.79	Nucleoli
IPI00017617	P17844	Probable ATP-dependent RNA helicase DDX5[a,b]	459	69,618	16	22.5	0.65	0.46	0.55	0.55	0.10	LKRD 0.91	Nucleoli
IPI00007765	P38646	Stress-70 protein, mitochondrial precursor	374	73,920	9	12.5	0.84	0.71	0.79	0.78	0.07	LKEE 0.91	Nucleoli
IPI00411937	O00567	Nucleolar protein Nop56[a]	159	66,408	8	9.3	0.73		0.53	0.63	0.14	LKKE 0.91	Nucleoli
IPI00220644	P14618	Isoform M1 of pyruvate kinase isozymes M1/M2	491	58,538	10	22.4	0.67	0.6	0.61	0.63	0.04	IKKP 0.84	Cytosol
IPI00290770	Q5SZY0	Chaperonin containing TCP1, subunit 3 isoform b	324	60,994	7	11.2	0.63		0.37	0.50	0.18	LKPD 0.91	Nucleus
IPI00304596	Q15233	Non-POU domain-containing octamer-binding protein[a]	259	54,311	6	14	0.76	0.77		0.77	0.01	AKVE 0.79	Nucleoli
IPI00440493	P25705	ATP synthase subunit α, mitochondrial precursor	491	59,828	13	21.9	0.79	0.69	0.81	0.76	0.06	MKLE 0.80	Mitochondrion
IPI00216049	Q5T6W2	Isoform 1 of heterogeneous nuclear ribonucleoprotein K[b]	398	51,230	9	20.5	0.73		0.84	0.79	0.08	GKPD 0.67	Nucleus
IPI00011200	O43175	D-3-Phosphoglycerate dehydrogenase	254	57,356	5	10.5	0.63		0.6	0.62	0.02	GKWE 0.67	Cytosol
IPI00303476	P06576	ATP synthase subunit β, mitochondrial precursor	435	56,525	7	18.7	0.82	0.71	0.69	0.74	0.07	IKIP 0.84	Nucleoli
IPI00218343	Q9BQE3	Tubulin α-6 chain[b]	427	50,548	8	20.9	0.7	0.49	0.66	0.62	0.11	VKCD 0.93	Nucleoli
IPI00032140	P05454	Serpin H1 precursor	327	46,525	7	19.4	0.46	0.38	0.22	0.35	0.12	VKKP 0.82	Endoplasmic reticulum
IPI00000875	P26641	Elongation factor 1-γ[b]	300	50,429	6	11.7	0.73	0.74	0.48	0.65	0.15	AKEE 0.79	Nucleoli
IPI00328328	Q14240	Isoform 1 of eukaryotic initiation factor 4A-II	216	46,601	4	11.5	0.67	0.51	0.31	0.50	0.18	VKEE 0.93	Nucleoli
IPI00021440	P63261	Actin, cytoplasmic 2	867	42,108	22	40.8	0.76		0.56	0.66	0.14	LKYP 0.80	Cytosol
IPI00549248	P06748	Isoform 1 of nucleophosmin[b]	356	32,611	13	17.7	0.73		0.48	0.61	0.18	LKAD 0.91	Nucleoli
IPI00553164	P08865	40 S ribosomal protein SA	247	32,947	6	16.3	0.74		0.83	0.79	0.06	MKEE 0.80	Nucleoli
IPI00455315	P07355	Annexin A2	536	38,808	15	44	0.74	0.48	0.66	0.63	0.13	VKGD 0.93	Nucleoli
IPI00217466	P16402	Histone H1.3	368	22,336	7	34.4	0.86		0.83	0.85	0.02	VKKP 0.82	Nucleoli
IPI00219018	P04406	Glyceraldehyde-3-phosphate dehydrogenase	323	36,201	8	25.4	0.84	0.76	0.13	0.58	0.39	VKAE 0.93	Nucleoli
IPI00220740	P06748	Isoform 2 of nucleophosmin[b]	247	29,617	6	13.6	0.68		0.48	0.58	0.14	LKAD 0.91	Nucleoli
IPI00215965	P09651	Isoform A1-B of heterogeneous nuclear ribonucleoprotein A1	165	38,936	3	11.8	0.86		0.63	0.75	0.16	IKED 0.94	Nucleoli
IPI00219217	P07195	L-Lactate dehydrogenase B chain	376	36,900	9	25.7	0.73	0.51		0.62	0.16	LKGE 0.91, LKDD 0.91	Cytosol
IPI00419880	P61247	40 S ribosomal protein S3a	342	30,154	9	32.6	0.64		0.65	0.65	0.01	VKAP 0.82	Nucleoli
IPI00030179	P18124	60 S ribosomal protein L7[a]	296	29,264	8	30.6	0.7	0.63		0.67	0.05	None	Nucleoli
IPI00329801	P08758	Annexin A5	234	35,971	5	15.6	0.71	0.81		0.76	0.07	IKGD 0.94, LKSE 0.91	Nucleoli
IPI00012772	P62917	60 S ribosomal protein L8[a]	126	28,235	4	16.7	0.73	0.6	0.35	0.56	0.19	VKLP 0.82	Nucleoli
IPI00021840	P62753	40 S ribosomal protein S6	120	28,834	2	8	0.64		0.38	0.51	0.18	VKKG 0.76	Nucleoli
IPI00018534	Q99880	Histone H2B type 1-L[b]	375	13,944	9	45.2	0.81		0.75	0.78	0.04	None	Nucleoli
IPI00026272	P04908	Histone H2A type 1-B[b]	214	14,127	6	37.7	0.68		0.72	0.70	0.03	None	Nucleoli
IPI00013296	P62269	40 S ribosomal protein S18	172	17,708	3	25	0.75		0.58	0.67	0.12	VKDG 0.76	Nucleoli
IPI00221092	P62249	40 S ribosomal protein S16	148	16,549	4	26	0.74		0.64	0.69	0.07	VKGG 0.76	Nucleoli

MCP MOLECULAR & CELLULAR PROTEOMICS ASBMB

TABLE I—*continued*

IPI accession number	Swiss-Prot accession number	Protein name	Protein score	Protein mass	Matched peptides	Protein coverage	H/L ratio			Average	S.D.	SUMO prediction sites	Subcellular localization
				Da		%	Experiment I	Experiment II	Experiment III				
IPI00026271	P62263	40 S ribosomal protein S14	136	16,434	2	17.9	0.66	0.54	0.61	0.60	0.06	VKAD 0.93	Nucleoli
IPI00453473	P62805	Histone H4[b]	473	11,360	13	57.3	0.81	0.76	0.76	0.78	0.03	None	Nucleus
IPI00328379	Q5T1N8	G-protein-signaling modulator 2	188	76,661	3	7.6		0.06	0.04	0.05	0.01	None	Cytoplasm
IPI00025721	Q9UNS2	COP9 signalosome complex subunit 3	53	47,873	1	2.8		0.32	0.5	0.41	0.13	None	Nucleus
IPI00003768	B2RDF2	Isoform 1 of Pescadillo homolog 1[b]	65	68,002	2	2.9		0.45	0.3	0.38	0.11	LKLE 0.91	Nucleoli
IPI00742682	P12270	Nucleoprotein TPR	355	267,290	8	4.1		0.57	0.46	0.52	0.08	VKLE 0.93	Nucleus
IPI00024279	Q9H583	HEAT repeat-containing protein 1	393	242,370	10	4.9		0.57	0.64	0.61	0.05	IKEE 0.94	Nucleoli
IPI00003377	Q16629	Isoform 1 of splicing factor, arginine/serine-rich 7	44	27,366	2	3.8		0.69	0.48	0.59	0.15	GKGE 0.67	Nucleus

[a] *In vitro* identified SUMO-1 targets.
[b] Known SUMO-1 targets.

the 100 identified proteins is available as supplemental Table S2. 23 of the identified proteins overlapped with the *in vivo* identified targets and belong to protein families as small nuclear ribonucleoproteins, hnRNPs, ribosomal proteins, DNA/RNA-binding proteins, and elongation factors. Moreover 22 SUMO-1 targets identified in this study, labeled by Footnote b (Table I), have been found previously in other SUMO-1 target protein screens supporting the validity of our strategy (48–51). Examples of known SUMO-1 target proteins are heterogeneous nuclear ribonucleoproteins such as hnRNPs K and M and the DEAD box family of RNA helicases, such as Ddx5, an interactor of transcription factors, that in its sumoylated form favors the recruitment of co-repressor thus repressing transcription (52, 53). Other known SUMO-1 targets, also identified in this study, are DNA topoisomerase II, SWI/SNF protein, and histone H4 (54–56).

The presence of a sumoylation consensus motif was determined in the 78 putative SUMO-1 target proteins using SUMOPlot as shown in Table I. A total of 330 consensus sumoylation motif were found in 70 of 78 (90% of total) identified proteins. Considering the frequency of SUMO-1 sites in the Swiss-Prot database (57), the p value was estimated to be $6.13e-10$ by the equation of hypergeometric distribution (58) indicating that proteins listed in Table I are indeed enriched in the sumoylation consensus motif, thus supporting the validity of the strategy adopted to identify endogenous SUMO-1 target proteins.

Identification of Novel SUMO-1 Target Proteins—To assess the sumoylation of novel SUMO-1 targets, we performed *in vitro* sumoylation reactions. It is known that several histones are sumoylated in yeast, but there is no evidence of this modification in mammals except for histone H4 (58, 59). An enriched fraction of histones was incubated in the presence of His-SUMO-1, Ubc9, Aos1/Uba2, inorganic pyrophosphatase, and ATP for 1 h at room temperature. The same reaction buffer devoid of His-SUMO-1 was used as control. Moreover the mixture was incubated without histones as a further control. Proteins were separated by SDS-PAGE and analyzed by Western blot with anti-SUMO-1 antibody. As shown in Fig. 7*A*, there is an evident band at 45 kDa appearing only after the reaction with SUMO-1. The corresponding band was in-gel digested and identified by LC-MS/MS as SUMO-1 and histone H1 (supplemental Table S3). This is in accordance with the molecular mass of the complex. Moreover purified histone H3 was also incubated in the presence (or absence as control) of the reaction buffer described above for 1 h at 37 °C, and the mixture was incubated without histone H3 as control of the reaction. Proteins were size-separated by SDS-PAGE and blotted to membranes, and sumoylated histone H3 was detected by anti-histone H3 antibody. As shown in Fig. 7*B*, there is an evident band at about 35 kDa due to histone H3 bound to one molecule of SUMO-1 that is not present in the control. The analysis of the Western blot with anti-SUMO-1 confirmed the transfer of the SUMO-1 moiety from Ubc9 to the sub-

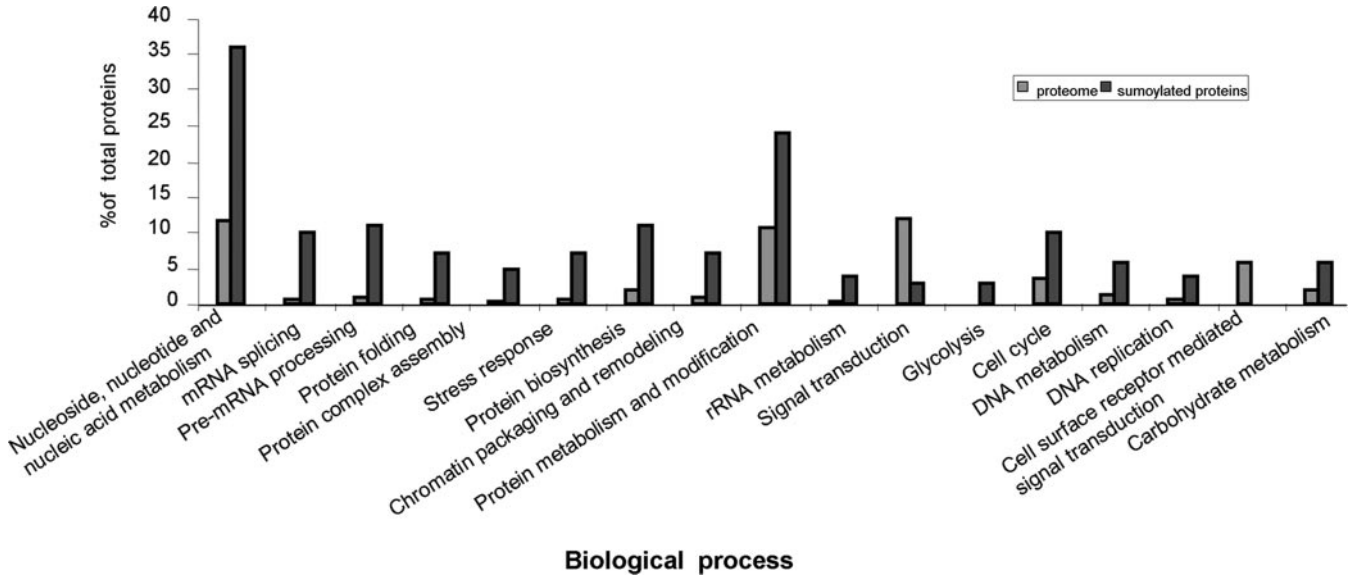

FIG. 5. **Biological process analysis.** Analysis was performed with the on-line software PANTHER using the data set reported in Table I. The *p* value was set at >0.05. The Bonferroni correction for multiple testings was used. Only categories with significant differences are shown.

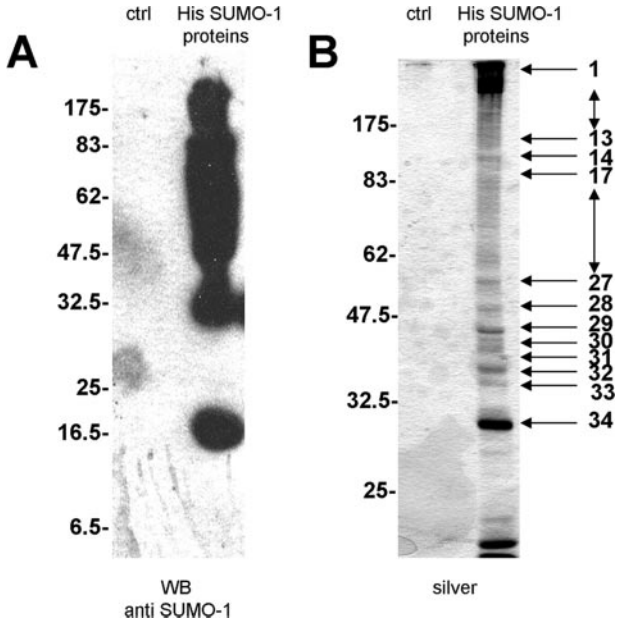

FIG. 6. **Purification of *in vitro* His-SUMO-1 target proteins.** An *in vitro* reaction of HeLa nuclear extract was performed with His-SUMO-1, which was previously bound to Ni^{2+} beads. The reaction mixture was obtained by incubating Ubc9, inorganic pyrophosphatase, and ATP in sumoylation buffer with and in the absence of SUMO-1 as control. *A*, anti-SUMO-1 Western blot (*WB*) of purified His-SUMO-1-conjugated proteins shows an enrichment of conjugated species. *B*, SDS-PAGE of purified His-SUMO-1 proteins stained by silver shows a very specific signal in the reaction mixture compared with the control (*ctrl*). The gel was excised in 34 slices for nLC-MS/MS analysis.

strate. The presence of sumoylated histone H3 was also confirmed by LC-MS/MS analysis of the band described above (supplemental Table S3).

Another novel SUMO-1 substrate, identified for the first time in this study, is the p160 Myb-binding protein 1A. p160 is mainly a nucleolar protein and, as reported in recent studies, may regulate ribosome biogenesis and Myb-dependent transcription (37, 60). To analyze the endogenous sumoylation of p160, NIH 3T3 cells were infected with p160-FLAG. Immunoprecipitation with anti-FLAG antibody and immunoblotting with anti-SUMO-1 indicated that p160 is indeed sumoylated (Fig. 7*C*).

DISCUSSION

As emerging from recent studies (61), SUMO-2/-3 modification may regulate the ubiquitin-proteasome system. One explanation is based on the discovery of novel ubiquitin ligases that mediate the targeting of sumoylated proteins to the proteasome (27). In this study we demonstrated that a cross-talk also exists between SUMO-1 and the ubiquitin-proteasome system. In contrast to SUMO-2/-3 proteins and ubiquitin itself, SUMO-1 does not form polychains. Such a peculiarity together with its endogenous low level in the cell makes this modification more difficult to detect. As a consequence, in several conditions, the effect of any stimulus, such as the inhibition of the proteasome system, seems to affect SUMO-1 much less than SUMO-2/3 (61). Interestingly we observed that upon MG132 treatment there is a complete redistribution of SUMO-1 targets from nuclear dots into nucleolar structures. This process was highly specific with respect to SUMO-1 behavior under several stress conditions suggesting that SUMO-1 may play a major role in the nucleolar compartment that is linked to the inhibition of the proteasome system. To better understand this biological event and overcome the problem of the low detection of SUMO-1, we focused our analysis on the nucleolus. Although a large frac-

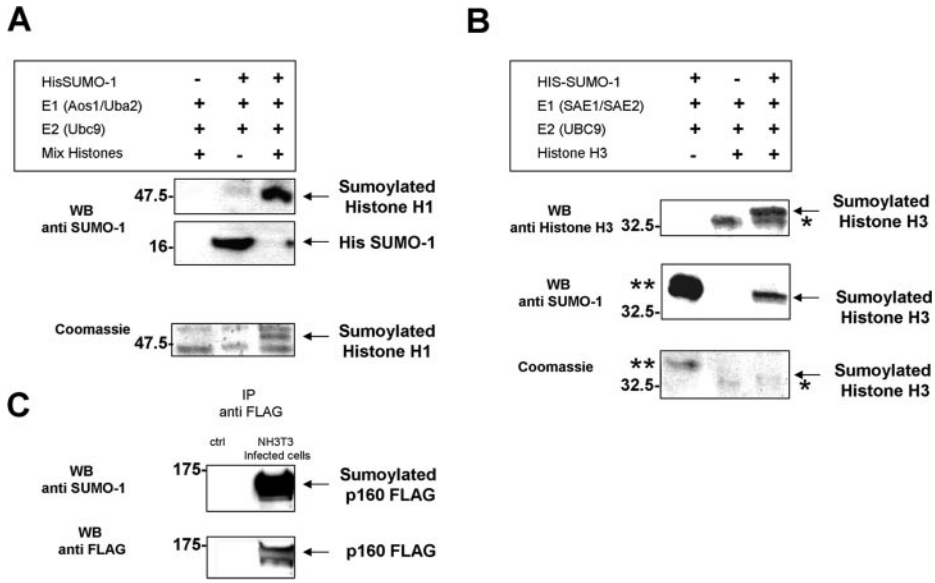

FIG. 7. **Novel SUMO-1 target identification.** *A*, histones mixture *in vitro* reaction. A mixture of calf thymus total histones was incubated in the presence or absence (as control) of His-SUMO-1, Ubc9, Aos1/Uba2, inorganic pyrophosphatase, and ATP in sumoylation buffer. The reaction mixture was analyzed by anti-SUMO-1 Western blot (*WB*) and SDS-PAGE. When SUMO-1 is added to the mixture, a new band of 45 kDa appears, and the amount of free SUMO-1 decreases indicating that SUMO-1 has been conjugated to one of the histones of the mixture. The Coomassie-stained band possibly corresponding to sumoylated histone was cut, trypsin-digested, and analyzed by nLC-MS/MS. This analysis identified histone H1.3 (supplemental Table S3) as the target of the sumoylation reaction. The identification of SUMO-1 protein confirms that the histone is sumoylated because the molecular mass of the band corresponds to the mass of the histone H1 plus SUMO-1. *B*, histone H3 *in vitro* reaction. Purified histone H3 was incubated in the presence or absence of SUMO-1 in the same reaction buffer described above, and the mixture was incubated without histone H3 as a control of the reaction. Proteins were separated by SDS-PAGE. Sumoylated histone H3 was detected by specific antibody as a band migrating at about 35 kDa, which was not present in the control. Western blot with anti-SUMO-1 confirms the transfer of SUMO-1 to the substrate. The sumoylation of histone H3 was also confirmed by nLC-MS/MS analysis of the band described above. * indicates a probable histone H3 dimer; ** indicates the complex Ubc9-SUMO-1. *C*, endogenous sumoylation of p160. NIH 3T3 cells were infected with p160-FLAG retrovirus. Immunoprecipitation (*IP*) with anti-FLAG affinity resin and immunoblotting with anti-SUMO-1 indicate that p160 is indeed sumoylated. Immunoprecipitation of not infected cells was used as control.

tion of SUMO-1 targets is supposed to reside in the nucleolus, no characterization of these proteins has been performed until now. In this work, we identified 193 SUMO-1 nucleolar targets by a proteomics approach. In addition, by quantitative analysis, we found that 78 of these substrates change their level of sumoylation in response to proteasome inhibition. These results confirm that there is a relationship between SUMO-1 and the ubiquitin-proteasome system suggesting that SUMO-1, together with ubiquitin, may ensure the integrity of nucleolar organization, acting as a second level of quality control in the regulation of ubiquitin-dependent proteolysis. To increase our knowledge of SUMO-1 in this compartment, we performed an analysis of the nature of the substrates influenced by proteasome inhibition and found proteins involved in ribosome biogenesis, protein complex assembly, RNA splicing and metabolism, chromatin packaging and remodeling, and DNA replication (Fig. 5). As already supposed in budding yeast (62), we found clustering of SUMO modification among subunits of multiprotein complexes indicating that this modification may have a specific cooperative activity. For example, concerning the regulation of ribosome biogenesis, we found several sumoylated elongation factors, such as hnRNP proteins, RNA helicases, and ribosomal subunits, suggesting that SUMO-1 modification may regulate the assembly of these macromolecular complexes. In particular, these substrates changed upon MG132 treatment, suggesting that SUMO-1 may target unassembled ribosomal proteins to the ubiquitin-proteasome system in analogy to what has been demonstrated in yeast (63). This is supported by the observation that a significant fraction of ribosomal proteins imported in the nucleolus is degraded and not assembled into the ribosome subunits (64). SUMO-1 could ensure the correct building of such large complexes by inhibiting incorrect interactions between proteins. The potential link between SUMO-1 and ubiquitin is further supported by the observation that among identified SUMO-1 targets ubiquitin was present with a high confidence score and high value of fold change after MG132 treatment in concordance with previous studies that have shown the presence of ubiquitin within nucleoli (65).

Another evidence of multisumoylated complexes comes from the identification of SUMO-1 targets such as lamin A, nucleophosmin, topoisomerase II, histone H1, p160 Myb-binding protein, and several ribosomal subunits, which belong to a macrocomplex containing CTCF (CCCTC-binding factor) protein (54, 60, 66–68). Some of these proteins are known to be sumoylated, whereas in this work we demonstrated that

p160 Myb-binding protein and Histones H1 and H3 are indeed modified by SUMO-1. These findings suggest that SUMO-1 modification may regulate the organization of this complex, participating in the transcription of rRNA genes, ribosome maturation, assembly, and transport. Recently it has also been demonstrated in *Drosophila* that ribosomal proteins interact with histone H1 on condensed chromatin, supporting the possibility that the association of ribosomal proteins on chromatin may be part of their assembly/maturation process (43).

In summary, we suggest that sumoylation may be one of the key regulators linking these cellular processes and that this post-translational modification plays an important and specific role in the ubiquitin-proteasome system. Further investigations on the biochemistry and cell biology of SUMO-1 target proteins identified in this work should help to elucidate further aspects of the inter-relationship of SUMO-1 target proteins and proteasome activity.

Acknowledgments—We thank Frauke Melchior for providing Ubc9 and Aos1/Uba2 cDNAs, Ronald Hay for SUMO-1 cDNA, and Emanuela Colombo for anti-nucleophosmin monoclonal antibody. We are grateful to Daniela Talarico for precious suggestions, scientific discussion, and technical advice.

* This work was supported by grants from Fondazione Cariplo (Project NoBEL to A. B.) and European Community Grant F2-2007-201681 (to F. B.).

S The on-line version of this article (available at http://www.mcponline.org) contains supplemental material.

§ Both authors contributed equally to this work.

‡‡ To whom correspondence should be addressed. Tel.: 39-26434927; Fax: 39-26434153; E-mail: bachi.angela@hsr.it.

REFERENCES

1. Zhang, F. P., Mikkonen, L., Toppari, J., Palvimo, J. J., Thesleff, I., and Jänne, O. A. (2008) Sumo-1 function is dispensable in normal mouse development. *Mol. Cell. Biol.* **28,** 5381–5390
2. Nacerddine, K., Lehembre, F., Bhaumik, M., Artus, J., Cohen-Tannoudji, M., Babinet, C., Pandolfi, P. P., and Dejean, A. (2005) The SUMO pathway is essential for nuclear integrity and chromosome segregation in mice. *Dev. Cell* **9,** 769–779
3. Gill, G. (2005) Something about SUMO inhibits transcription. *Curr. Opin. Genet. Dev.* **15,** 536–541
4. Wilson, V. G., and Heaton, P. R. (2008) Ubiquitin proteolytic system: focus on SUMO. *Expert Rev. Proteomics* **5,** 121–135
5. Geiss-Friedlander, R., and Melchior, F. (2007) Concepts in sumoylation: a decade on. *Nat. Rev. Mol. Cell Biol.* **8,** 947–956
6. Meulmeester, E., and Melchior, F. (2008) Cell biology: SUMO. *Nature* **452,** 709–711
7. Guo, D., Li, M., Zhang, Y., Yang, P., Eckenrode, S., Hopkins, D., Zheng, W., Purohit, S., Podolsky, R. H., Muir, A., Wang, J., Dong, Z., Brusko, T., Atkinson, M., Pozzilli, P., Zeidler, A., Raffel, L. J., Jacob, C. O., Park, Y., Serrano-Rios, M., Larrad, M. T., Zhang, Z., Garchon, H. J., Bach, J. F., Rotter, J. I., She, J. X., and Wang, C. Y. (2004) A functional variant of SUMO4, a new I kappa B alpha modifier, is associated with type 1 diabetes. *Nat. Genet.* **36,** 837–841
8. Melchior, F. (2000) SUMO—nonclassical ubiquitin. *Annu. Rev. Cell Dev. Biol.* **16,** 591–626
9. Lapenta, V., Chiurazzi, P., van der Spek, P., Pizzuti, A., Hanaoka, F., and Brahe, C. (1997) SMT3A, a human homologue of the S. cerevisiae SMT3 gene, maps to chromosome 21qter and defines a novel gene family. *Genomics* **40,** 362–366
10. Johnson, E. S. (2004) Protein modification by SUMO. *Annu. Rev. Biochem.* **73,** 355–382
11. Martin, S., Wilkinson, K. A., Nishimune, A., and Henley, J. M. (2007) Emerging extranuclear roles of protein SUMOylation in neuronal function and dysfunction. *Nat. Rev. Neurosci.* **8,** 948–959
12. Owerbach, D., McKay, E. M., Yeh, E. T., Gabbay, K. H., and Bohren, K. M. (2005) A proline-90 residue unique to SUMO-4 prevents maturation and sumoylation. *Biochem. Biophys. Res. Commun.* **337,** 517–520
13. Tatham, M. H., Jaffray, E., Vaughan, O. A., Desterro, J. M., Botting, C. H., Naismith, J. H., and Hay, R. T. (2001) Polymeric chains of SUMO-2 and SUMO-3 are conjugated to protein substrates by SAE1/SAE2 and Ubc9. *J. Biol. Chem.* **276,** 35368–35374
14. Matic, I., van Hagen, M., Schimmel, J., Macek, B., Ogg, S. C., Tatham, M. H., Hay, R. T., Lamond, A. I., Mann, M., and Vertegaal, A. C. (2008) In vivo identification of human small ubiquitin-like modifier polymerization sites by high accuracy mass spectrometry and an in vitro to in vivo strategy. *Mol. Cell. Proteomics* **7,** 132–144
15. Hietakangas, V., Anckar, J., Blomster, H. A., Fujimoto, M., Palvimo, J. J., Nakai, A., and Sistonen, L. (2006) PDSM, a motif for phosphorylation-dependent SUMO modification. *Proc. Natl. Acad. Sci. U.S.A.* **103,** 45–50
16. Zhao, J. (2007) Sumoylation regulates diverse biological processes. *Cell. Mol. Life Sci.* **64,** 3017–3033
17. Ulrich, H. D. (2005) Mutual interactions between the SUMO and ubiquitin systems: a plea of no contest. *Trends Cell Biol.* **15,** 525–532
18. Pickart, C. M., and Fushman, D. (2004) Polyubiquitin chains: polymeric protein signals. *Curr. Opin. Chem. Biol.* **8,** 610–616
19. Desterro, J. M., Rodriguez, M. S., and Hay, R. T. (1998) SUMO-1 modification of IkappaBalpha inhibits NF-kappaB activation. *Mol. Cell* **2,** 233–239
20. Huang, T. T., Wuerzberger-Davis, S. M., Wu, Z. H., and Miyamoto, S. (2003) Sequential modification of NEMO/IKKgamma by SUMO-1 and ubiquitin mediates NF-kappaB activation by genotoxic stress. *Cell* **115,** 565–576
21. Shimada, K., Suzuki, N., Ono, Y., Tanaka, K., Maeno, M., and Ito, K. (2008) Ubc9 promotes the stability of Smad4 and the nuclear accumulation of Smad1 in osteoblast-like Saos-2 cells. *Bone* **42,** 886–893
22. Lee, P. S., Chang, C., Liu, D., and Derynck, R. (2003) Sumoylation of Smad4, the common Smad mediator of transforming growth factor-beta family signaling. *J. Biol. Chem.* **278,** 27853–27863
23. Hay, R. T. (2005) SUMO: a history of modification. *Mol. Cell* **18,** 1–12
24. Gill, G. (2004) SUMO and ubiquitin in the nucleus: different functions, similar mechanisms? *Genes Dev.* **18,** 2046–2059
25. Bailey, D., and O'Hare, P. (2005) Comparison of the SUMO1 and ubiquitin conjugation pathways during the inhibition of proteasome activity with evidence of SUMO1 recycling. *Biochem. J.* **392,** 271–281
26. Mattsson, K., Pokrovskaja, K., Kiss, C., Klein, G., and Szekely, L. (2001) Proteins associated with the promyelocytic leukemia gene product (PML)-containing nuclear body move to the nucleolus upon inhibition of proteasome-dependent protein degradation. *Proc. Natl. Acad. Sci. U.S.A.* **98,** 1012–1017
27. Tatham, M. H., Geoffroy, M. C., Shen, L., Plechanovova, A., Hattersley, N., Jaffray, E. G., Palvimo, J. J., and Hay, R. T. (2008) RNF4 is a poly-SUMO-specific E3 ubiquitin ligase required for arsenic-induced PML degradation. *Nat. Cell Biol.* **10,** 538–546
28. Ong, S. E., Blagoev, B., Kratchmarova, I., Kristensen, D. B., Steen, H., Pandey, A., and Mann, M. (2002) Stable isotope labeling by amino acids in cell culture, SILAC, as a simple and accurate approach to expression proteomics. *Mol. Cell. Proteomics* **1,** 376–386
29. Ong, S. E., Foster, L. J., and Mann, M. (2003) Mass spectrometric-based approaches in quantitative proteomics. *Methods* **29,** 124–130
30. Ong, S. E., and Mann, M. (2007) Stable isotope labeling by amino acids in cell culture for quantitative proteomics. *Methods Mol. Biol.* **359,** 37–52
31. Desterro, J. M., Thomson, J., and Hay, R. T. (1997) Ubc9 conjugates SUMO but not ubiquitin. *FEBS Lett.* **417,** 297–300
32. Pichler, A., Gast, A., Seeler, J. S., Dejean, A., and Melchior, F. (2002) The nucleoporin RanBP2 has SUMO1 E3 ligase activity. *Cell* **108,** 109–120
33. Cordell, J. L., Pulford, K. A., Bigerna, B., Roncador, G., Banham, A., Colombo, E., Pelicci, P. G., Mason, D. Y., and Falini, B. (1999) Detection of normal and chimeric nucleophosmin in human cells. *Blood* **93,** 632–642
34. Bush, H., Muramatsu, M., Adams, H., Steele, W. J., Liau, M. C., and Smetana, K. (1963) Isolation of nucleoli. *Exp. Cell Res.* **24,** 150–163
35. Andersen, J. S., Lam, Y. W., Leung, A. K., Ong, S. E., Lyon, C. E., Lamond,

A. I., and Mann, M. (2005) Nucleolar proteome dynamics. *Nature* **433,** 77–83
36. Leung, A. K., Trinkle-Mulcahy, L., Lam, Y. W., Andersen, J. S., Mann, M., and Lamond, A. I. (2006) NOPdb: Nucleolar Proteome Database. *Nucleic Acids Res.* **34,** D218–D220
37. Díaz, V. M., Mori, S., Longobardi, E., Menendez, G., Ferrai, C., Keough, R. A., Bachi, A., and Blasi, F. (2007) p160 Myb-binding protein interacts with Prep1 and inhibits its transcriptional activity. *Mol. Cell. Biol.* **27,** 7981–7990
38. Dignam, J. D., Lebovitz, R. M., and Roeder, R. G. (1983) Accurate transcription initiation by RNA polymerase II in soluble extract from isolated mammalian nuclei. *Nucleic Acids Res.* **11,** 1475–1489
39. Okuma, T., Honda, R., Ichikawa, G., Tsumagari, N., and Yasuda, H. (1999) In vitro SUMO-1 modification requires two enzymatic steps, E1 and E2. *Biochem. Biophys. Res. Commun.* **254,** 693–698
40. Shevchenko, A., Wilm, M., Vorm, O., and Mann, M. (1996) Mass spectrometric sequencing of proteins silver-stained polyacrylamide gels. *Anal. Chem.* **68,** 850–858
41. Nesvizhskii, A. I., Keller, A., Kolker, E., and Aebersold, R. (2003) A statistical model for identifying proteins by tandem mass spectrometry. *Anal. Chem.* **75,** 4646–4658
42. Zhang, J., Li, J., Liu, X., Xie, H., Zhu, Y., and He, F. (2008) A nonparametric model for quality control of database search results in shotgun proteomics. *BMC Bioinformatics* **9,** 29
43. Ni, J. Q., Liu, L. P., Hess, D., Rietdorf, J., and Sun, F. L. (2006) Drosophila ribosomal proteins are associated with linker histone H1 and suppress gene transcription. *Genes Dev.* **20,** 1959–1973
44. Cox, J., and Mann, M. (2008) MaxQuant enables high peptide identification rates, individualized p.p.b.-range mass accuracies and proteome-wide protein quantification. *Nat. Biotechnol.* **26,** 1367–1372
45. Eskiw, C. H., Dellaire, G., and Bazett-Jones, D. P. (2004) Chromatin contributes to structural integrity of promyelocytic leukemia bodies through a SUMO-1-independent mechanism. *J. Biol. Chem.* **279,** 9577–9585
46. Bossis, G., and Melchior, F. (2006) Regulation of SUMOylation by reversible oxidation of SUMO conjugating enzymes. *Mol. Cell* **21,** 349–357
47. Cascio, P., Oliva, L., Cerruti, F., Mariani, E., Pasqualetto, E., Cenci, S., and Sitia, R. (2008) Dampening Ab responses using proteasome inhibitors following in vivo B cell activation. *Eur. J. Immunol.* **38,** 658–667
48. Zhao, X., and Blobel, G. (2005) A SUMO ligase is part of a nuclear multiprotein complex that affects D and chromosomal organization. *Proc. Natl. Acad. Sci. U.S.A.* **102,** 4777–4782
49. Pountney, D. L., Raftery, M. J., Chegini, F., Blumbergs, P. C., and Gai, W. P. (2008) NSF, Unc-18–1, dynamin-1 and HSP90 are inclusion body components in neuronal intranuclear inclusion disease identified by anti-SUMO-1-immunocapture. *Acta Neuropathol.* **116,** 603–614
50. Moran, D. M., Shen, H., and Maki, C. G. (2009) Puromycin-based vectors promote a ROS-dependent recruitment of PML to nuclear inclusions enriched with HSP70 and proteasomes. *BMC Cell Biol.* **10,** 32
51. Kinoshita, Y., Jarell, A. D., Flaman, J. M., Foltz, G., Schuster, J., Sopher, B. L., Irvin, D. K., Kanning, K., Kornblum, H. I., Nelson, P. S., Hieter, P., and Morrison, R. S. (2001) Pescadillo, a novel cell cycle regulatory protein abnormally expressed in malignant cells. *J. Biol. Chem.* **276,** 6656–6665
52. Vassileva, M. T., and Matunis, M. J. (2004) SUMO modification of heterogeneous nuclear ribonucleoproteins. *Mol. Cell. Biol.* **24,** 3623–3632
53. Jacobs, A. M., Nicol, S. M., Hislop, R. G., Jaffray, E. G., Hay, R. T., and Fuller-Pace, F. V. (2007) SUMO modification of the DEAD box protein p68 modulates its transcriptional activity and promotes its interaction with HDAC1. *Oncogene* **26,** 5866–5876
54. Dawlaty, M. M., Malureanu, L., Jeganathan, K. B., Kao, E., Sustmann, C., Tahk, S., Shuai, K., Grosschedl, R., and van Deursen, J. M. (2008) Resolution of sister centromeres requires RanBP2-mediated SUMOylation of topoisomerase IIalpha. *Cell* **133,** 103–115
55. Rosas-Acosta, G., Russell, W. K., Deyrieux, A., Russell, D. H., and Wilson, V. G. (2005) A universal strategy for proteomic studies of SUMO and other ubiquitin-like modifiers. *Mol. Cell. Proteomics* **4,** 56–72
56. Shiio, Y., and Eisenman, R. N. (2003) Histone sumoylation is associated with transcriptional repression. *Proc. Natl. Acad. Sci. U.S.A.* **100,** 13225–13230
57. Vertegaal, A. C., Andersen, J. S., Ogg, S. C., Hay, R. T., Mann, M., and Lamond, A. I. (2006) Distinct and overlapping sets of SUMO-1 and SUMO-2 target proteins revealed by quantitative proteomics. *Mol. Cell. Proteomics.* **5,** 2298–2310
58. Zhou, F., Xue, Y., Lu, H., Chen, G., and Yao, X. (2005) A genome-wide analysis of sumoylation-related biological processes and functions in human nucleus. *FEBS Lett.* **579,** 3369–3375
59. Nathan, D., Ingvarsdottir, K., Sterner, D. E., Bylebyl, G. R., Dokmanovic, M., Dorsey, J. A., Whelan, K. A., Krsmanovic, M., Lane, W. S., Meluh, P. B., Johnson, E. S., and Berger, S. L. (2006) Histone sumoylation is a negative regulator in Saccharomyces cerevisiae and shows dynamic interplay with positive-acting histone modifications. *Genes Dev.* **20,** 966–976
60. Yamauchi, T., Keough, R. A., Gonda, T. J., and Ishii, S. (2008) Ribosomal stress induces processing of Mybbp1a and its translocation from the nucleolus to the nucleoplasm. *Genes Cell* **13,** 27–39
61. Schimmel, J., Larsen, K. M., Matic, I., van Hagen, M., Cox, J., Mann, M., Andersen, J. S., and Vertegaal, A. C. (2008) The ubiquitin-proteasome system is a key component of the SUMO-2/3 cycle. *Mol. Cell. Proteomics* **7,** 2107–2122
62. Takahashi, Y., Dulev, S., Liu, X., Hiller, N. J., Zhao, X., and Strunnikov, A. (2008) Cooperation of sumoylated chromosomal proteins in rDNA maintenance. *PLoS Genet.* **4,** e1000215
63. Panse, V. G., Kressler, D., Pauli, A., Petfalski, E., Gnädig, M., Tollervey, D., and Hurt, E. (2006) Formation and nuclear export of preribosomes are functionally linked to the small-ubiquitin-related modifier pathway. *Traffic* **7,** 1311–1321
64. Lam, Y. W., Lamond, A. I., Mann, M., and Andersen, J. S. (2007) Analysis of nucleolar protein dynamics reveals the nuclear degradation of ribosomal proteins. *Curr. Biol.* **17,** 749–760
65. Stavreva, D. A., Kawasaki, M., Dundr, M., Koberna, K., Müller, W. G., Tsujimura-Takahashi, T., Komatsu, W., Hayano, T., Isobe, T., Raska, I., Misteli, T., Takahashi, N., and McNally, J. G. (2006) Potential roles for ubiquitin and the proteasome during ribosome biogenesis. *Mol. Cell. Biol.* **26,** 5131–5145
66. Zhang, Y. Q., and Sarge, K. D. (2008) Sumoylation regulates lamin A function and is lost in lamin A mutants associated with familial cardiomyopathies. *J. Cell Biol.* **182,** 35–39
67. Tago, K., Chiocca, S., and Sherr, C. J. (2005) Sumoylation induced by the Arf tumor suppressor: a p53-independent function. *Proc. Natl. Acad. Sci. U.S.A.* **102,** 7689–7694
68. MacPherson, M. J., Beatty, L. G., Zhou, W., Du, M., and Sadowski, P. D. (2009) The CTCF insulator protein is posttranslationally modified by SUMO. *Mol. Cell. Biol.* **29,** 714–725